

Sliding right into disaster: Left-to-right sliding windows leak

Daniel J. Bernstein², Joachim Breitner³, Daniel Genkin^{3,4},
Leon Groot Bruinderink¹, Nadia Heninger³, Tanja Lange¹,
Christine van Vredendaal¹, Yuval Yarom⁵

¹ Technische Universiteit Eindhoven, Netherlands
L.Groot.Bruinderink@tue.nl, tanja@hyperelliptic.org,
c.v.vredendaal@tue.nl

² University of Illinois at Chicago, USA
djb@cr.yp.to

³ University of Pennsylvania, USA
{joachim,danielg3,nadiah}@cis.upenn.edu

⁴ University of Maryland, USA

⁵ University of Adelaide and Data61, CSIRO, Australia
yval@cs.adelaide.edu.au

Abstract. It is well known that constant-time implementations of modular exponentiation cannot use sliding windows. However, software libraries such as Libgcrypt, used by GnuPG, continue to use sliding windows. It is widely believed that, even if the complete pattern of squarings and multiplications is observed through a side-channel attack, the number of exponent bits leaked is not sufficient to carry out a full key-recovery attack against RSA. Specifically, 4-bit sliding windows leak only 40% of the bits, and 5-bit sliding windows leak only 33% of the bits.

In this paper we demonstrate a complete break of RSA-1024 as implemented in Libgcrypt. Our attack makes essential use of the fact that Libgcrypt uses the left-to-right method for computing the sliding-window expansion. We show for the first time that the direction of the encoding matters: the pattern of squarings and multiplications in left-to-right sliding windows leaks significantly more information about the exponent than right-to-left. We show how to extend the Heninger-Shacham algorithm for partial key reconstruction to make use of this information and obtain a very efficient full key recovery for RSA-1024. For RSA-2048 our attack is efficient for 13% of keys.

Keywords: left-to-right sliding windows, collision entropy, cache attack, Flush+Reload, RSA-CRT.

1 Introduction

Modular exponentiation in cryptosystems such as RSA is typically performed starting from the most significant bit (MSB) in a left-to-right manner. More efficient implementations use precomputed values to decrease the number of

multiplivEcations. Typically these windowing methods are described in a right-to-left manner, starting the recoding of the exponent from the least significant bit (LSB), leading to the potential disadvantage that the exponent has to be parsed twice: once for the recoding and once of the exponentiation.

This motivated researchers to develop left-to-right analogues of the integer recoding methods that can be integrated directly with left-to-right exponentiation methods. For example, the only method for sliding-window exponentiation in the Handbook of Applied Cryptography [17, Chap 14.6] is the left-to-right version of the algorithm. Doche [8] writes “To enable ‘on the fly’ recoding, which is particularly interesting for hardware applications” in reference to Joye and Yen’s [15] left-to-right algorithm.

Given these endorsements, it is no surprise that many implementations chose a left-to-right method of recoding the exponent. For example, Libgcrypt implements a left-to-right exponentiation with integrated recoding. Libgcrypt is part of the GnuPG code base [2], and is used in particular by GnuPG 2.x, which is a very popular implementation of the OpenPGP standard [6] for applications such as encrypted email and files. Libgcrypt is also used by various other applications; see [1] for a list of frontends.

It is known that exponentiation using sliding-window methods leaks information, specifically the pattern of squarings and multiplications, through cache-based side-channel attacks. However, it is commonly believed that for window width w only about a fraction $2/(w + 1)$ bits would leak: each window has 1 bit known to be 1, and each gap has on average 1 bit known to be 0, compared to $w + 1$ bits occupied on average by the window and the gap.

Libgcrypt 1.7.6, the last version at the time of writing this paper, resists the attacks of [10, 16], because the Libgcrypt maintainers accepted patches to protect against chosen-ciphertext attacks and to hide timings obtained from loading precomputed elements. However, the maintainers refused a patch to switch from sliding windows to fixed windows; they said that this was unnecessary to stop the attacks. RSA-1024 in Libgcrypt uses the CRT method and $w = 4$, which according to the common belief reveals only 40% of all bits, too few to use the key-recovery attack [12] by Heninger and Shacham. RSA-2048 uses CRT and $w = 5$, which according to the common belief reveals only 33% of all bits.

1.1 Contributions

In this paper we show that the common belief is incorrect for the left-to-right recoding: this recoding actually leaks many more bits. An attacker learning the location of multiplications in the left-to-right squarings-and-multiplications sequence can recover the key for RSA-1024 with CRT and $w = 4$ in a search through fewer than 10000 candidates for most keys, and fewer than 1000000 candidates for practically all keys. Note that RSA-1024 and RSA-1280 remain widely deployed in some applications, such as DNSSEC. Scaling up to RSA-2048 does not stop our attack: we show that 13% of all RSA-2048 keys with CRT and $w = 5$ are vulnerable to our method after a search through 2000000 candidates.

We analyze the reasons that left-to-right leaks more bits than right-to-left and extensive experiments show the effectiveness of this attack. We further improve

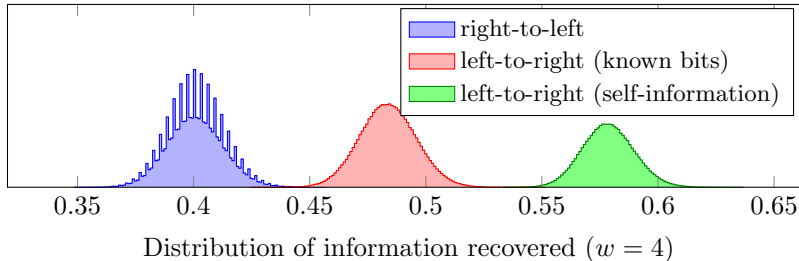


Fig. 1: The sequence of squares and multiplies of left-to-right windowed exponentiation contains much more information about the exponent than from exponentiation in the other direction, both in the form of known bits (red) and information-theoretic bits (green). Recovering close to 50% of the information about the key allows an efficient full key recovery attack.

the algorithm by Heninger and Shacham to make use of less readily available information to attack RSA-2048, and prove that our extended algorithm efficiently recovers the full key when the side channel leaks data with a *self-information* rate greater than $1/2$.

To illustrate the real-world applicability of this attack, we demonstrate how to obtain the required side-channel data (the pattern of squarings and multiplications) from the modular-exponentiation routine in Libgcrypt version 1.7.6 using a Flush+Reload [25, 26] cache-timing attack that monitors the target’s cache-access patterns. The attack combines a small number of traces (at most 20) using the same secret RSA key, and does not depend on further frontend details.

1.2 Targeted Software and Current Status

Software and Hardware. We target Libgcrypt version 1.7.6 which is the latest version at the time of writing this paper. We compiled Libgcrypt using GCC version 4.4.7 using `-O2` optimization level. We performed the attack on an HP-Elite 8300 desktop machine, running Centos 6.8 with kernel version 3.18.41-20. The machine has a 4-core Intel i5-3470 processor, running at 3.2 GHz, with 8 GiB of DDR3-1600 CL-11 memory.

Current Status. Using the practice of responsible disclosure, we disclosed this issue to the Libgcrypt maintainers and are working with them to produce and validate patch for mitigating our attack. The vulnerability has been assigned CVE-2017-7526. A new version of Libgcrypt will be released simultaneously with the publication of this paper.

2 Preliminaries

2.1 RSA-CRT

RSA signature key generation is done by generating two random primes p, q . The public key is then set to be (e, N) where e is a (fixed) public exponent and $N = pq$. The private key is set to be (d, p, q) where $ed \equiv 1 \pmod{\phi(n)}$ and

Algorithm 1 Sliding window modular exponentiation.

Input: Three integers b , d and p where $d_n \cdots d_1$ is a windowed form of d .**Output:** $a \equiv b^d \pmod{p}$.

```

1: procedure MOD_EXP( $b, d, p$ )
2:    $b_1 \leftarrow b, b_2 \leftarrow b^2 \pmod{p}, a \leftarrow 1$ 
3:   for  $i \leftarrow 1$  to  $2^{w-1} - 1$  do            $\triangleright$  precompute table of small powers of  $b$ 
4:      $b_{2i+1} \leftarrow b_{2i-1} \cdot b_2 \pmod{p}$ 
5:   for  $i \leftarrow n$  to  $1$  do
6:      $a \leftarrow a \cdot a \pmod{p}$ 
7:     if  $d_i \neq 0$  then
8:        $a \leftarrow a \cdot b_{d_i} \pmod{p}$ 
9:   return  $a$ 

```

$\phi(n) = (p-1)(q-1)$. RSA signature of a message m is done by computing $s = h(m)^d \pmod{N}$ where h is a padded cryptographically secure hash function. Signature verification is done by computing $z = s^e \pmod{N}$ and verifying that z equals $h(m)$. A common optimization for RSA signatures is based on the Chinese Remainder Theorem (CRT). Instead of directly computing $s = h(m)^d \pmod{N}$ directly, the signer computes $s_p = h(m)^{d_p} \pmod{p}$, $s_q = h(m)^{d_q} \pmod{q}$ (where d_p and d_q are derived from the secret key) and then combines s_p and s_q into s using the CRT. The computations of s_p and s_q work with half-size operands and have half-length exponents, leading to a speedup of a factor 2–4.

2.2 Sliding Window Modular Exponentiation

In order to compute an RSA signature (more specifically the values of s_p and s_q defined above), two modular exponentiation operations must be performed. A modular exponentiation operation gets as inputs base b , exponent d , and modulus p and outputs $b^d \pmod{p}$. A common method used by cryptographic implementations is the sliding window method, which assumes that the exponent d is given in a special representation, the windowed form. For a window size parameter w , the windowed form of d is a sequence of digits $d_{n-1} \cdots d_0$ such that $d = \sum_{i=0}^{n-1} d_i 2^i$ and d_i is either 0 or an odd number between 1 and $2^w - 1$.

Algorithm 1 performs the sliding window exponentiation method, assuming that the exponent is given in a windowed form, in two steps: It first precomputes the values of $b^1 \pmod{p}, b^3 \pmod{p}, \dots, b^{2^w-1} \pmod{p}$ for odd powers of b . Then, the algorithm scans the digits of d from the most significant bit (MSB) to the least significant bit (LSB). For every digit, the algorithm performs a squaring operation (**Line 6**) on the accumulator variable a . Finally, for every non-zero digit of d , the algorithm performs a multiplication (**Line 8**).

2.3 Sliding Window Conversion

The representation of a number d in (sliding) windows is not unique, even for a fixed value of w . In particular, the binary representation of d is a valid window form. However, since each non-zero digit requires a costly multiplication operation, it is desirable to reduce the number of non-zero digits in d 's sliding windows.

Right-to-Left Sliding Windows. One approach to computing d 's sliding windows (with fewer of non-zero digits) scans d 's binary representation from the least significant bit (LSB) to the most significant bit (MSB) and generates d 's sliding windows from the least significant digit (right) to the most significant digit (left). For every clear bit, a zero digit is appended to the left of the windowed form. For each set bit, a non-zero digit is appended whose value is the w -bit integer ending at the current bit. The next $w - 1$ digits in the windowed form are set to be zero digits. The scan resumes from the leftmost bit unused so far. Finally, any leading zeroes in the window form are truncated.

For example, let $w = 3$, and $d = 181$, which is $\underline{1} \underline{0} \underline{1} \underline{1} \underline{0} \underline{1} \underline{0} \underline{1}$ in binary. The windows are underlined. This yields the sliding window form 10030005.

Left-to-Right Windowed Form. An alternative approach is the left-to-right windowed form, which scans the bits of d the most to least significant bit and the windowed form is generated from the most significant digit to the least significant one. Similar to the right-to-left form, for every scanned clear bit a zero digit is appended to the right of the windowed form. When a set bit is encountered, since we require from digits to be odd, the algorithm cannot simply set the digit to be the w -bit integer starting at the current bit. Instead, it looks for the longest integer u that has its most significant bit at the current bit, terminates in a set bit, and its number of bits k is at most w bits long. The algorithm sets the next $k - 1$ digits in the windowed form to be zero, sets the subsequent digit to be u and resumes the scan from the next bit unused so far. As before, leading zeroes in the sliding window form are truncated.

Using the $d = 181$ and $w = 3$ example, the left-to-right sliding windows are $\underline{1} \underline{0} \underline{1} \underline{1} \underline{0} \underline{1} \underline{0} \underline{1}$ and the corresponding windowed form is 500501

Left-to-Right vs. Right-to-Left. While both the methods produce a windowed form whose average density (the ratio between the non-zero digits and the total form length) is about $1/(w + 1)$, generating the windowed form using the right-to-left method guarantees that every non-zero digit is followed by at least $w - 1$ zero digits. This is contrast to the left-to-right method, where two non-zero digits can be as close as adjacent. As explained in [Section 3](#), such consecutive non-zero digits can be observed by the attacker, aiding key recovery for sliding window exponentiations using the left-to-right windowed form.

2.4 GnuPG's Sliding Window Exponentiation

While producing the right-to-left sliding window form requires a dedicated procedure, the left-to-right form can be generated “on-the-fly” during the exponentiation algorithm, combining the generation of the expansion and the exponentiation itself in one go. Consequently, the left-to-right sliding window form [17, Algorithm 14.85], shown in [Algorithm 2](#), is the prevalent method used by many implementations, including GnuPG.

Every iteration of the main loop ([Line 6](#)) constructs the next non-zero digit u of the windowed form by locating the location i of leftmost set bit of d which was not previously handled ([Line 8](#)) and then removing the trailing zeroes from $d_i \cdots d_{i-w+1}$. It appends the squaring operations needed in order to handle

Algorithm 2 Left-to-right sliding window modular exponentiation.**Input:** Three integers b , d and p where $d_n \cdots d_1$ is the binary representation of d .**Output:** $a \equiv b^d \pmod{p}$.

```

1: procedure MOD_EXP( $b, d, p$ )
2:    $b_1 \leftarrow b, b_2 \leftarrow b^2, a \leftarrow 1, z \leftarrow 0$ 
3:   for  $i \leftarrow 1$  to  $2^{w-1} - 1$  do           ▷ precompute table of small odd powers of  $b$ 
4:      $b_{2i+1} \leftarrow b_{2i-1} \cdot b_2 \pmod{p}$ 
5:    $i \leftarrow n$ 
6:   while  $i \neq 1$  do                               ▷ main loop for computing  $b^d \pmod{p}$ 
7:      $z \leftarrow z + \text{COUNT\_LEADING\_ZEROS}(d_i \cdots d_1)$ 
8:      $i \leftarrow i - z$                                ▷  $i$  is the leftmost unscanned set bit of  $d$ 
9:      $l \leftarrow \min(i, w)$ 
10:     $u \leftarrow d_i \cdots d_{i-l+1}$ 
11:     $t \leftarrow \text{COUNT\_TRAILING\_ZEROS}(u)$ 
12:     $u \leftarrow \text{SHIFT\_RIGHT}(u, t)$            ▷ remove trailing zeroes by shifting  $u$  to the right
13:    for  $j \leftarrow 1$  to  $z + l - t$  do
14:       $a \leftarrow a \cdot a \pmod{p}$ 
15:       $a \leftarrow a \cdot b_u \pmod{p}$            ▷ notice that  $u$  is always odd
16:       $i \leftarrow i - l$ 
17:       $z \leftarrow t$ 
18:    return  $a$ 

```

the zero windowed form digits preceding u (Line 13) before performing the multiplication operation using u as the index to the precomputation table (thus handling u), and keeping track of trailing zeroes in z .

3 Sliding Right versus Sliding Left Analysis

In this section, we show how to recover some bits of the secret exponents, assuming that the attacker has access to the square-and-multiply sequence performed by Algorithm 2. We show that more bits can be found by applying this approach to the square-and-multiply sequence of the left-to-right method compared to that of the right-to-left method. At high level, our approach consists of two main steps. In the first step, we show how to directly recover some of the bits of the exponent by analyzing the sequence of squaring and multiplication operations performed by Algorithm 2. This step shows that we are capable of directly recovering an average of 48% of the bits of d_p and d_q for 1024-bit RSA with $w = 4$, the window size used by Libgcrypt for 1024-bit RSA. However, the number of remaining unknown bits required for a full key recovery attack is still too large to brute force. In Section 3.4 we show that applying a modified version of the techniques of [12] allows us to recover the remaining exponent bits and obtain the full private key, if at least 50% of the bits are recovered.

3.1 Analyzing the Square and Multiply Sequence

Assume the attacker has access to the sequence $S \in \{s, m\}^*$ corresponding to the sequence of square and multiply operations performed by Algorithm 2

$$\begin{aligned}
 \text{Rule 0:} & \quad \underline{x} \rightarrow \underline{1} \\
 \text{Rule 1:} & \quad \underline{1x^i 1x^{w-i-1}} \rightarrow \underline{1x^i 10^{w-i-1}} \quad \text{for } i = 0, \dots, w-2 \\
 \text{Rule 2:} & \quad \underline{xxx11} \rightarrow \underline{1xx11} \\
 \text{Rule 3:} & \quad \underline{1x^i x^{w-1} 1} \rightarrow \underline{10^i x^{w-1} 1} \quad \text{for } i > 0
 \end{aligned}$$

Fig. 2: Rules to deduce known bits from a square-and-multiply sequence

executed on some exponent d . Notice that the squaring operation (Line 13) is performed once per bit of d , while the multiplication operation is performed only for some exponent bits. Thus, we can represent the attacker's knowledge about S as a sequence $s \in \{0, 1, \underline{1}, x, \underline{x}\}^*$ where 0, 1 indicate known bits of d , x denotes an unknown bit and the positions of multiplications are underlined. For $y \in \{0, 1, \underline{1}, x, \underline{x}\}$ we denote by y^i the i -times repetition of y times.

Since at the start of the analysis all the bits are unknown, we convert S to the sequence s as follows: every sm turns into a \underline{x} , all remaining s into x . As a running example, the sequence of squares and multiplies $S = smsssssssmsssssm$ is converted into $D_1 = \underline{xxxxxxxxxxxxxx}$.

To obtain bits of d from S_1 , the attacker applies the rewrite rules in Figure 2.

Rule 0: Multiplication bits. Because every digit in the windowed form is odd, a multiplication always happens at bits that are set.

Applied to D_1 we obtain $D_2 = \underline{1xxxxxx11xxxx1}$.

Rule 1: Trailing zeros. The algorithm tries to include as many set bits as possible in one digit of the windowed form. So when two multiplications are fewer than w bits apart, we learn that there were no further set bits available to include in the digit corresponding to the second multiplication. Rule 1 sets the following bits to zero accordingly.

Applied to D_2 we obtain $D_3 = \underline{1xxxxxx11000x1}$.

Rule 2: Leading one. If we find two immediately consecutive multiplications, it is clear that as the algorithm was building the left digit, there were no trailing zeroes in $u = d_i \cdots d_{i-l+1}$, i.e. $t = 0$ in Line 11. This tells us the precise location of d_i , which we know is set.

Applied to D_3 we obtain $D_4 = \underline{1xxx1xx11000x1}$.

Rule 3: Leading zeroes. Every set bit of d is included in a non-zero digit of the windowed form, so it is at most $w - 1$ bits to the left of a multiplication. If two consecutive multiplications are more than w bits apart, we know that there are zeroes in between.

Applied to D_4 we obtain $D_5 = \underline{10001xx11000x1}$.

Larger Example. Consider the bit string

0100001111100101001100110101001100001100011111100011100100001001.

The corresponding sequence of square and multiply operations (using $w = 4$) evolves as follows as we apply the rules:

```

xxxxxxxxxxxxxxxxxxxxxxxxxxxxxxxxxxxxxxxxxxxxxxxxxxxxxxxxxxxxxxxxxxxxxxxx
x1xxxxxxxx1xxx1xxx1xxx1xx1xxxx11xxxxxxxx1xxxxxxxx1x1xxxx1xx1xxxxxxxx1
x100xxxxxxxx1xxx1xxx1xxx1xx10xxx11000xx10xxxxx1x100xxx1xx10xxxxxx1
x100xxxxxxxx1xxx1xxx1xxx1xx101xx11000xx10xxxxx1x100xxx1xx10xxxxxx1
x10000xxx1xxx10xxx1xxx1xx101xx11000xx1000xxx1x100xxx1xx10000xxx1.

```

Out of the 64 bits, 34 become known through this analysis.

Iterative Application. The previous examples shows that by applying rules iteratively, we can discover a few more bits. In particular, for a window where a leading one is recovered (Rule 2), one may learn the leading bit of the preceding window. Iterating Rule 2 in the example above gives 3 more known leading bits:

```

x10000xxx1xxx101xx11xx11x101xx11000xx1000xxx1x100xxx1xx10000xxx1.

```

This iterative behavior is hard to analyze and occurs rarely in practice. Therefore the following analysis disregards it. Note that the algorithm of Section 3.4 does use the additional bits.

3.2 Analyzing Recovery Rules

In this section we analyze the number of bits we are theoretically expected to recover using Rules 0–3 described in the previous section. The analysis applies to general window size w and the bit string length n .

Renewal processes with rewards. We model the number of bits recovered as a renewal reward process [22]. A renewal process is associated with interarrival times $\underline{X} = (X_1, X_2, \dots)$ where the X_i are independent, identically distributed and non-negative variables with a common distribution function F and mean μ . Let

$$S_n = \sum_{i=1}^n X_i, \quad n \in \mathbb{N},$$

where $\underline{S} = (0, S_1, S_2, \dots)$ is the sequence of arrival times and

$$N_t = \sum_{n=1}^{\infty} \mathbf{1}(S_n \leq t), \quad t \in \mathbb{R}^+$$

is the associated counting process. Now let $\underline{Y} = (Y_1, Y_2, \dots)$ be an i.i.d. sequence associated with \underline{X} in the sense that Y_i is the reward for the interarrival X_i . Note that even though both \underline{X} and \underline{Y} are i.i.d., X_i and Y_i can be dependent. Then the stochastic process

$$R_t = \sum_{i=1}^{N_t} Y_i, \quad t \in \mathbb{R}^+,$$

is a renewal reward process. The function $r(t) = \mathbb{E}(R_t)$ is the renewal reward function. We can now state the *renewal reward theorem* [18]. Since $\mu_X < \infty$ and $\mu_Y < \infty$ we have for the renewal reward process

$$\begin{aligned} R_t/t &\rightarrow \mu_Y/\mu_X \text{ as } t \rightarrow \infty \text{ with probability 1,} \\ r(t)/t &\rightarrow \mu_Y/\mu_X \text{ as } t \rightarrow \infty. \end{aligned}$$

This is related to our attack in the following way. The n bit locations of the bit string form an interval of integers $[1, n]$, labeling the leftmost bit as 1. We set $X_1 = b + w - 1$, where b is the location of the first bit set to 1, that is, the left boundary of the first window. Then the left boundary of the next window is independent of the first $b + w - 1$ bits. The renewal process examines each window independently. For each window X_i we gain information about *at least* the multiplication bit. This is the reward Y_i associated with X_i . The renewal reward theorem now implies that for bit strings of length n , the expected number of recovered bits will converge to $\frac{n\mu_Y}{\mu_X}$.

Recovered bit probabilities. In the remainder of this section we analyze the expected number of bits that are recovered (the reward) in some number of bits (the renewal length) by the rules of Section 3.1. Then by calculating the probability of each of these rules' occurrence, we can compute the overall number of recovered bits by using the renewal reward theorem. Note that Rule 0 (the bits set to $\underline{1}$) can be incorporated into the other rules by increasing their recovered bits by one.

Rule 1: Trailing zeroes. The first rule applies to short windows. Recall that we call a window a "short window" whenever the length between two multiplications is less than $w - 1$.

Let $0 \leq j \leq w - 2$ denote the length between two multiplications. (A length of $w - 1$ is a full-size window.) The probability of a short window depends on these j bits, as well as $w - 1$ bits after the multiplication: the multiplication bit should be the right-most 1-bit in the window. The following theorem (which we prove in the full version of this paper) gives the probability of a short window.

Theorem 1. *Let X be an interarrival time. Then the probability that $X = w$ and we have a short window with reward $Y = w - j$, $0 \leq j \leq w - 2$ is*

$$p_j = \frac{1 + \sum_{i=1}^j 2^{2i-1}}{2^{j+w}}$$

We see in the proof that the bits $y_{w-j-1}, \dots, y_{w-2}$ can take any values. Also since bit $y_{w-j-2} = 0$ is known, we have a renewal at this point where future bits are independent.

Rule 2: Leading one. As explained in Section 3.1, this rule means that when after renewal an ultra-short window occurs (a 1 followed by $w - 1$ zeroes) we get an extra bit of information about the previous window. The exception to this rule is if the previous window was also an ultra-short window. In this case the $\underline{1}$ of the window is at the location of the multiplication bit we would have learned and therefore we do not get extra information. As seen in the previous section, an ultra-short window occurs with probability $p_0 = 1/2^w$. If an ultra-short window occurs after the current window with window-size $1 \leq j \leq w - 1$, we therefore recover $(w - j) + 1$ bits (all bits of the current window plus 1 for the leading bit) with probability $p_j p_0$ and $(w - j)$ with probability $p_j(1 - p_0)$.

Rule 3: Leading zeroes. The last way in which extra bits can be recovered is the leading zeroes. If a window of size $w - d$ is preceded by more than d

zeroes, then we can recover the excess zeroes. Let X_0 be a random variable of the length of a bit string of zeros until the first 1 is encountered. Then X_0 is geometrically distributed with $p = 1/2$. So $\mathbb{P}[X_0 = k] = (1/2)^k \cdot (1/2) = (1/2)^{k+1}$. This distribution has mean $\mu_X = 1$.

Let X_w be a random variable representing the length of the bit string from the first 1 that was encountered until the multiplication bit. For general window length of w , we have

$$\mathbb{P}[X_w = k] = \begin{cases} \frac{1}{2^{w-1}} & k = 1 \\ \frac{1}{2^{w-k+1}} & k > 1 \end{cases}$$

Now the distribution of the full bit string is the sum of the variables X_0 and X_w . We have that $\mathbb{P}[X_0 + X_w = k] = \sum_{i=1}^{\min(k,w)} \mathbb{P}[X_w = i] \cdot \mathbb{P}[X_0 = k - i]$. Notice that this rule only recovers bits if the gap between two multiplications is at least $w - 1$. This means that these cases are independent of Rule 1.

There is a small caveat in this analysis: the renewal length is unclear. In the case that we have a sequence of zeroes followed by a short window of size $j < w$, we are implicitly conditioning on the $w - j$ bits that follow. This means we cannot simply renew after the the 1 and since we also cannot distinguish between a short and regular window size, we also cannot know how much information we have on the bits that follow.

We solve this by introducing an upper and lower bound. For the upper bound the recovered bits remains as above and the renewal at $X_0 + w$. This is an obvious upper bound. This means that for a sequence of zeroes followed by a short window of size j , we assume a probability of 1 of recovering information on the $w - j$ bits that follow the sequence. We get an average recovered bits of

$$\bar{R} = \sum_{k=w}^{\infty} \sum_{i=1}^{\min(k,w)} (k - i + 1) \cdot \mathbb{P}[X_w = i] \cdot \mathbb{P}[X_0 = k - i],$$

and a renewal length of

$$\bar{N} = \sum_{k=w}^{\infty} \sum_{i=1}^{\min(k,w)} (k + w - i) \cdot \mathbb{P}[X_w = i] \cdot \mathbb{P}[X_0 = k - i].$$

For the lower bound we could instead assume a probability of 0 of recovering information on the $w - j$ bits. We can however get a tighter bound by observing that the bits that follow this rule are more likely a 0 than a 1 and we are more likely to recover a 0 at the start of a new window than we are a 0. Therefore bound the renewal at $X_0 + X_w$ and throw away the extra information. Similar formulas can be derived for the lower bounds \underline{R} and \underline{N} .

From this, we can calculate the expected renewal length for fixed w , by summing over all possible renewal lengths with corresponding probabilities. We can do the same for the expected number of recovered bits per renewal. Finally, we are interested in the expected total number of recovered bits in a n -bit string. We calculate this by taking an average number of renewals (by dividing n by

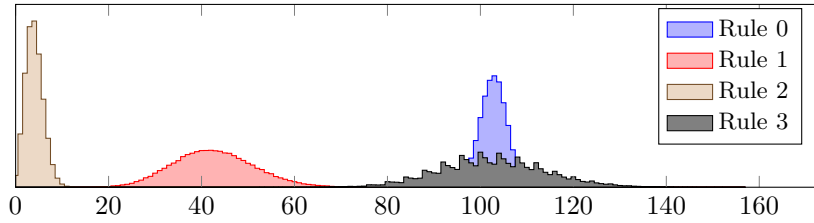


Fig. 3: We generated 100,000 random 512-bit strings and generated the square and multiply sequence with $w = 4$. We then applied Rules 0–3 successively to recover bits of the original string. We plot the distribution of the number of recovered bits in our experiments.

the expected renewal length) and multiply this with the number of recovered bits per window. Since we have upper and lower bounds for both the renewal length and recovered bits for Rule 3, we also get lower and upper bounds for the expected total number of recovered bits.

Recovered Bits for Right-to-Left. The analysis of bit recovery for right-to-left exponentiation is simpler. The bit string is an alternation of X_0 and X_w (see Rule 3), where $X_w = w$ and X_0 is geometrically distributed with $p = 1/2$. Therefore the expected renewal length N and the expected reward R are

$$N = \sum_{i=0}^{\infty} (w + i) \cdot \mathbb{P}[X_0 = i] = w + 1 \quad \text{and} \quad R = \sum_{i=0}^{\infty} (1 + i) \cdot \mathbb{P}[X_0 = i] = 2.$$

Then by the renewal reward theorem, we expect to recover $\frac{2n}{w+1}$ bits.

3.3 Experimental Verification

To experimentally validate our analysis, we sampled n -bit binary strings uniformly at random and used [Algorithm 2](#) to derive the square and multiply sequence. We then applied Rules 0–3 from [Section 3.1](#) to extract known bits.

Case $n = 512, w = 4$. [Figure 1](#) shows the total fraction of bits learned for right-to-left exponentiation compared to left-to-right exponentiation, for $w = 4$, over 1,000,000 experiments with $w = 4$ and $n = 512$, corresponding to our target Libgcrypt’s implementation for 1024-bit RSA. On average we learned 251 bits, or 49%, for left-to-right exponentiation with 512-bit exponents. This is between our computed lower bound of $\beta_L = 245$ (from a renewal length of $\bar{N} = 4.67$ bits and reward of 2.24 bits on average per renewal) and upper bound $\beta_U = 258$ (from a renewal length of $\bar{N} = 4.90$ bits and reward of 2.47 bits per renewal). The average number of recovered bits for right-to-left exponentiation is $204 \approx \frac{2n}{w+1}$ bits, or 40%, as expected.

[Figure 3](#) shows the distribution of the number of new bits learned for each rule with left-to-right exponentiation by successively applying Rules 0–3 for 100,000 exponents. Both Rule 0 and Rule 3 contribute about $205 \approx \frac{2n}{w+1}$ bits, which is equal both to our theoretical analysis and is also the number of bits learned from

the right-to-left exponentiation. The spikes visible in Rule 3 are due to the fact that we know that any least significant bits occurring after the last window must be 0, and we credit these bits learned to Rule 3. The number of bits learned from this final step is equal to $n \bmod w$, leading to small spikes at intervals of w bits.

Case $n = 1024, w = 5$. For $n = 1024$ and $w = 5$, corresponding to Libcrypt’s implementation of 2048-bit RSA, we recover 41.5% of bits on average using Rules 0–3. This is between our lower bound of $\beta_L = 412$ (from a lower bound average renewal length of $\underline{N} = 5.67$ bits, and expected 2.29 bits on average per renewal) and upper bound of $\beta_U = 436$ (from an average renewal length of $\bar{N} = 5.89$ bits with an average reward of 2.51 bits per renewal). Note that the reward per renewal is about the same as in the first case ($n = 512, w = 4$), but the average renewal length is higher. This means that we win fewer bits for this case.

3.4 Full RSA Key Recovery from Known Bits

Once we have used the recovered sequence of squares and multiplies to derive some information about the bits of the Chinese remainder theorem coefficients $d_p = d \bmod (p - 1)$ and $d_q = d \bmod (q - 1)$, we can use a modified version of the branch and prune algorithm of Heninger and Shacham [12] to recover the remaining unknown bits of these exponents to recover the full private key.

The algorithm will recover the values d_p and d_q from partial information. In order to do so, we use the integer forms of the RSA equations

$$\begin{aligned} ed_p &= 1 + k_p(p - 1) \\ ed_q &= 1 + k_q(q - 1) \end{aligned}$$

which these values satisfy for positive integers $k_p, k_q < e$.

RSA Coefficient Recovery. As described in [13, 27], k_p and k_q are initially unknown, but are related via the equation $(k_p - 1)(k_q - 1) \equiv k_p k_q N \bmod e$. Thus we need to try at most e pairs of k_p, k_q . In the most common case, $e = 65537$. As described in [27], incorrect values of k_p, k_q quickly result in no solutions.

LSB-Side Branch and Prune Algorithm. At the beginning of the algorithm, we have deduced some bits of d_p and d_q using Rules 0–3. Given candidate values for k_p and k_q , we can then apply the approach of [12] to recover successive bits of the key starting from the least significant bits. Our algorithm does a depth-first search over the unknown bits of d_p, d_q, p , and q . At the i th least significant bit, we have generated a candidate solution for bits $0 \dots i - 1$ of each of our unknown values. We then verify the equations

$$\begin{aligned} ed_p &= 1 + k_p(p - 1) \bmod 2^i \\ ed_q &= 1 + k_q(q - 1) \bmod 2^i \\ pq &= N \bmod 2^i \end{aligned} \tag{1}$$

and prune a candidate solution if any of these equations is not satisfied.

Analysis. Heuristically, we expect this approach to be efficient when we know more than 50% of bits for d_p and d_q , distributed uniformly at random. [12, 19] We

also expect the running time to grow exponentially in the number of unknown bits when we know many fewer than 50% of the bits. From the analysis of Rules 0–3 above, we expect to recover 48% of the bits. While the sequence of recovered bits is not, strictly speaking, uniformly random since it is derived using deterministic rules, the experimental performance of the algorithm matched that of a random sequence.

Experimental Evaluation for $w = 4$. We ran 500,000 trial key recovery attempts for randomly generated d_p and d_q with 1024-bit RSA and $w = 4$. For a given trial, if the branching process passed 1,000,000 candidates examined without finding a solution, we abandoned the attempt. Experimentally, we recover more than 50% of the bits 32% of the time, and successfully recovered the key in 28% of our trials. For 50% or 512 bits known, the median number of examined candidates was 182,738. We recovered 501 bits on average in our trials using Rules 0–3; at this level the median number of candidates was above 1 million.

Experimental Evaluation for $w = 5$. We experimented with this algorithm for 2048-bit RSA, with $w = 5$. The number of bits that can be derived unconditionally using Rules 0–3 is around 41% on average, below the threshold where we expect the Heninger-Shacham algorithm to terminate for 1024-bit exponents. The algorithm did not yield any successful key recovery trials at this size.

4 RSA Key Recovery from Squares and Multiplies

The sequence of squares and multiplies encodes additional information about the secret exponent that does not translate directly into knowledge of particular bits. In this section, we give a new algorithm that exploits this additional information by recovering RSA keys directly from the square-and-multiply sequence. This gives a significant speed improvement over the key recovery algorithm described in Section 3.4, and brings an attack against $w = 5$ within feasible range.

4.1 Pruning from Squares and Multiplies

Our new algorithm generates a depth-first tree of candidate solutions for the secret exponents, and prunes a candidate solution if it could not have produced the ground-truth square-and-multiply sequence obtained by the side-channel attack. Let $SM(d) = s$ be the deterministic function that maps a bit string d to a sequence of squares and multiplies $s \in \{s, m\}^*$.

In the beginning of the algorithm, we assume we have ground truth square-and-multiply sequences s_p and s_q corresponding to the unknown CRT coefficients d_p and d_q . We begin by recovering the coefficients k_p and k_q using brute force as described in Section 3.4. We will then iteratively produce candidate solutions for the bits of d_p and d_q by generating a depth-first search tree of candidates satisfying Equations 1 starting at the least significant bits. We will attempt to prune candidate solutions for d_p or d_q at bit locations i for which we know the precise state of Algorithm 2 from the corresponding square and multiply sequence s , namely when element i of s is a multiply or begins a sequence of w squares. To test an i -bit candidate exponent d_i , we compare $s' = SM(d_i)$ to positions 0 through $i - 1$ of s , and prune d_i if the sequences do not match exactly.

4.2 Algorithm Analysis

We analyze the performance of this algorithm by computing the expected number of candidate solutions examined by the algorithm before it recovers a full key. Our analysis was inspired by the information-theoretic analysis of [19], but we had to develop a new approach to capture the present scenario.

Let $p_s = \Pr[\text{SM}(d_i) = s]$ be the probability that a fixed square-and-multiply sequences s is observed for a uniformly random i -bit sequence d_i . This defines the probability distribution D_i of square-and-multiply sequences for i -bit inputs.

In order to understand how much information a sequence s leaks about an exponent, we will use the *self-information*, defined as $I_s = -\log p_s$. This is the analogue of the number of bits known for the algorithm given in Section 3.4. As with the bit count, we can express the number of candidate solutions that generate s in terms of I_s : $\#\{d \mid \text{SM}(d) = s\} = 2^i p_s = 2^i 2^{-I_s}$. For a given sequence s , let I_i denote the self-information of the least significant i bits.

Theorem 2 (Heuristic). *If for the square-and-multiply sequences s_{p_i} and s_{q_i} , we have $I_i > i/2$ for almost all i , then the algorithm described in Section 4.1 runs in expected linear time in the number of bits of the exponent.*

Proof (Sketch). In addition pruning based on s , the algorithm also prunes by verifying the RSA equations up to bit position i . Let $\text{RSA}_i(d_p, d_q) = 1$ if $(ed_p - 1 + k_p)(ed_q - 1 + k_q) = k_p k_q N \pmod{2^i}$ and 0 otherwise. For random (incorrect) candidates d_{p_i} and d_{q_i} , $\Pr[\text{RSA}_i(d_{p_i}, d_{q_i})] = 1/2^i$.

As in [12], we heuristically assume that, once a bit has been guessed wrong, the set of satisfying candidates for d_{p_i} and d_{q_i} behave randomly and independently with respect to the RSA equation at bit position i .

Consider an incorrect guess at the first bit. We wish to bound the candidates examined before the decision is pruned. The number of incorrect candidates satisfying the square-and-multiply constraints and the RSA equation at bit i is

$$\begin{aligned} \#\{d_{p_i}, d_{q_i}\} &\leq \#\{d_{p_i} \mid \text{SM}(d_{p_i}) = s_{p_i}\} \cdot \#\{d_{q_i} \mid \text{SM}(d_{q_i}) = s_{q_i}\} \cdot \Pr[\text{RSA}_i(d_{p_i}, d_{q_i})] \\ &= 2^i 2^{-I_i} \cdot 2^i 2^{-I_i} \cdot 2^{-i} = 2^{i-2I_i} \leq 2^{i \cdot (1-2c)} \end{aligned}$$

with $I_i/i \geq c$ for some $c > 1/2$.

In total, there are $\sum_i \#\{d_{p_i}, d_{q_i}\} \leq \sum_i 2^{i \cdot (1-2c)} \leq 1/(1 - 2^{1-2c})$ candidates.

But *any* of the n bits can be guessed wrongly, each producing a branch of that size. Therefore, the total search tree has at most $n \cdot (1 + \frac{1}{1-2^{1-2c}})$ nodes.

A similar argument also tells us about the expected size of the search tree, which depends on the *collision entropy* [21]

$$H_i = -\log \sum_{s \in \{\text{s,m}\}^i} p_s^2$$

of the distribution D_i of distinct square-and-multiply sequences. This is the log of the probability that two i -bit sequences chosen according to D_i are identical.

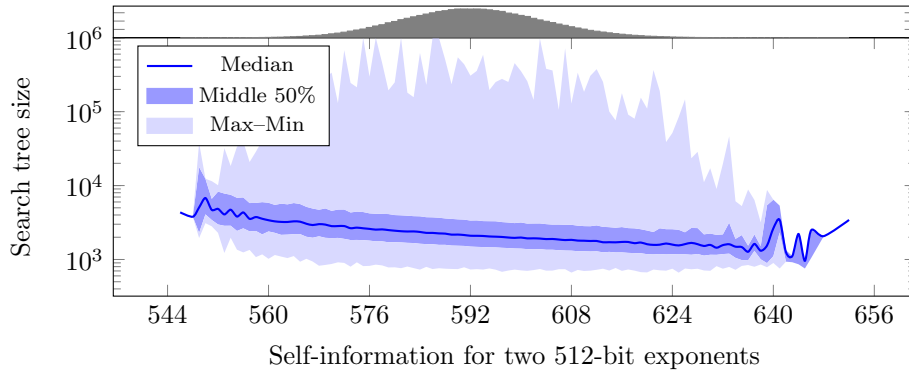


Fig. 4: We attempted 500,000 key recovery trials for randomly generated 1024-bit RSA keys with $w = 4$. We plot the distribution of the number of candidates tested by the algorithm against the self-information of the observed square-and-multiply sequences, measured in bits. The histogram above the plot shows the distribution of self-information across all the trials.

For our distribution D_i , the H_i are approximately linear in i . We can define the *collision entropy rate* $H = H_i/i$ and obtain an upper bound for the expected number of examined solutions, which we prove in the full version of the paper:

Theorem 3. *The expected total number of candidate solutions examined by Algorithm 2 for n -bit d_p and d_q is*

$$E \left[\sum_i \#\{d_{p_i}, d_{q_i}\} \right] \leq n \left(1 + \frac{1 - 2^{n \cdot (1-2H)}}{1 - 2^{1-2H}} \right).$$

Entropy calculations. We calculated the collision entropy rate by modeling the leak as a Markov chain. For $w = 4$, $H = 0.545$, and thus we expect Algorithm 2 to comfortably run in expected linear time. For $w = 5$, $H = 0.461$, and thus we expect the algorithm to successfully terminate on some fraction of inputs. We give more details on this computation in the full version of this paper.

4.3 Experimental Evaluation for $w = 4$

We ran 500,000 trials of our sequence-pruning algorithm for randomly generated d_p and d_q with 1024-bit RSA and plot the distribution of running times in Figure 4. For a given trial, if the branching process passed 1,000,000 candidates examined without finding a solution, we abandoned the attempt. For each trial square-and-multiply sequence s , we computed the number of bit sequences that could have generated it. From the average of this quantity over the 1 million exponents generated in our trial, the collision entropy rate in our experiments is $H = 0.547$, in line with our analytic computation above. The median self-information of the exponents generated in our trials was 295 bits; at this level the median number of candidates examined by the algorithm was 2,174. This can be

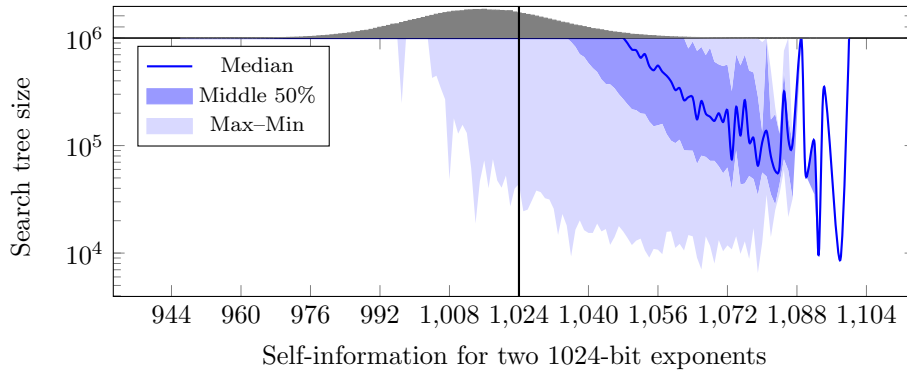


Fig. 5: We attempted 500,000 key recovery trials for randomly generated 2048-bit RSA keys with $w = 5$, and plot the distribution of search tree size by the self-information. The vertical line marks the 50% rate at which we expect the algorithm to be efficient.

directly compared to the 251 bits recovered in Section 3, since the self-information in that case is exactly the number of known bits in the exponent.

4.4 Experimental Evaluation for $w = 5$

We ran 500,000 trials of our sequence-pruning algorithm for 2048-bit RSA and $w = 5$ with randomly generated d_p and d_q and plot the distribution of running times in Figure 5. 8.6% of our experimental trials successfully recovered the key before hitting the panic threshold of 1 million tries. Increasing the allowed tree size to 2 million tries allowed us to recover the key in 13% of trials. We experimentally estimate a collision entropy rate $H = 0.464$, in line with our analytic computation. The median self-information for the exponents generated in our trials is 507 bits, significantly higher than the 420 bits that can be directly recovered using the analysis in Section 3.

5 Attacking Libgcrypt

In the previous section we showed how an attacker with access to the square-and-multiply sequence can recover the private RSA key. To complete the discussion we show how the attacker can obtain the square-and-multiply sequence.

5.1 The Side-Channel Attack

To demonstrate the vulnerability in Libgcrypt, we use the Flush+Reload attack [26]. The attack, which monitors shared memory locations for access by a victim, consists of two phases. The attacker first evicts a monitored location from the cache, typically using the x86 `clflush` instruction. He then waits for a short while, before measuring the time to access the monitored location. If the victim has accessed the memory location during the wait, the contents of the memory location will be cached, and the attacker's access will be fast. Otherwise, the

attacker causes the contents to be retrieved from the main memory and his access takes longer. By repeating the attack, the attacker creates a trace of the victim accesses to the monitored location over time. Flush+Reload has been used in the past to attack modular exponentiation [3, 26], as well as other cryptographic primitives [4, 5, 14, 20, 25] and non-cryptographic software [11, 29].

Mounting the Flush+Reload attack on Libgcrypt presents several challenges. First, as part of the defense against the attack of Yarom and Falkner [26], Libgcrypt uses the multiplication code to perform the squaring operation. While this is less efficient than using a dedicated code for squaring, the use of the same code means that we cannot identify the multiply operations by probing a separate multiply code. Instead we probe code locations that are used between the operations to identify the call site to the modular reduction.

The second challenge is achieving a sufficiently high temporal resolution. Prior side-channel attacks on implementations of modular exponentiation use large (1024–4096 bits) moduli [9, 10, 16, 26, 28], which facilitate side-channel attacks [23]. In this attack we target RSA-1024, which uses 512-bit moduli. The operations on these moduli are relatively fast, taking a total of less than 2500 cycles on average to compute a modular multiplication. To be able to distinguish events of this length, we must probe at least twice as fast, which is close to the limit of the Flush+Reload attack and would result in a high error rate [3]. We use the amplification attack of Allan et al. [3] to slow down the modular reduction. We target the code of the subtraction function used as part of the modular reduction. The attack increases the execution time of the modular reduction to over 30000 cycles.

Our third challenge is that even with amplification, there is a chance of missing a probe [3]. To reduce the probability of this happening, we probe two memory locations within the execution path of short code segments. The likelihood of missing both probes is small enough to allow high-quality traces.

Overall, we use the Flush+Reload attack to monitor seven victim code location. The monitored locations can be divided into three groups. To distinguish between the exponentiations Libgcrypt performs while signing, we monitor locations in the entry and exit of the exponentiation function. We also monitor a location in the loop that precomputes the multipliers to help identifying these multiplications. To trace individual modular multiplications, we monitor locations within the multiply and the modular reduction functions. Finally, to identify the multiplication by non-zero multipliers, we monitor locations in the code that conditionally copies the multiplier and in the entry to the main loop of the exponentiation. The former is accessed when Libgcrypt selects the multiplier before it performs the multiplication. The latter is accessed after the multiplication when the next iteration of the main loop starts. We repeatedly probe these locations once every 10000 cycles, allowing for 3–4 probes in each modular multiply or square operation.

5.2 Results

To mount the attack, we use the `FR-trace` software, included in the Mastik toolkit [24]. `FR-trace` provides a command-line interface for performing the

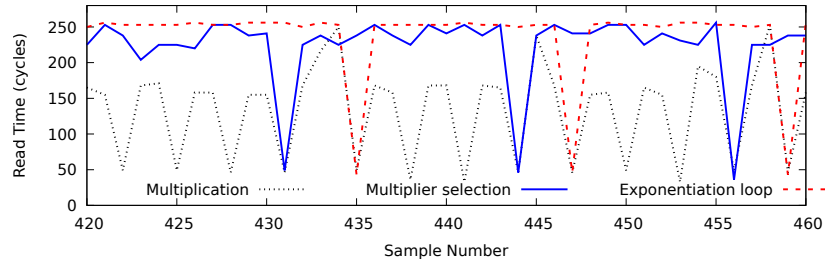


Fig. 6: Libgrypt Activity Trace.

Flush+Reload and the amplification attacks we require for recovering the square-and-multiply sequences of the Libgrypt exponentiation. **FR-trace** waits until there is activity in any of the monitored locations and collects a trace of the activity. Figure 6 shows a part of a collected activity trace.

Recall that the Flush+Reload attack identifies activity in a location by measuring the time it takes to read the contents of the location. Fast reads indicate activity. In the figure, monitored locations with read time below 100 cycles indicate that the location was active during the sample.

Because multiplications take an average 800 cycles, whereas our sample rate is once in 10000 cycles, most of the time activity in the multiplication code is contained within a single sample. In Figure 6 we see the multiplication operations as “dips” in the multiplication trace (dotted black).

Each multiplication operation is followed by a modular reduction. Our side-channel amplification attack “stretches” the execution of the modular reduction and it spans over more than 30000 cycles. Because none of the memory addresses traced in the figure is active during the modular reduction, we see gaps of 3–4 samples between periods of activity in any of the other monitored locations.

To distinguish between multiplications that use one of the precomputed multipliers and multiplications that square the accumulator by multiplying it with itself, we rely on activity in the multiplier selection and in the exponentiation loop locations. Before multiplying with a precomputed multiplier, the multiplier needs to be selected. Hence we would expect to see activity in the multiplier selection location just before starting the multiply, and due to the temporal granularity of the attack we are likely to see both events in the same sample. Similarly, after performing the multiplication and the modular reduction, we expect to see activity in the beginning of the main exponentiation loop. Again, due to attack granularity, this activity is likely to occur within the same sample as the following multiplication. Thus, because we see activity in the multiplier selection location during sample 431 and activity in the beginning of the exponentiation loop in the following multiplication (sample 435), we can conclude that the former multiplication is using one of the precomputed multipliers.

In the absence of errors, this allows us to completely recover the sequence of square and multiplies performed and with it, the positions of the non-zero digits in the windowed representation of the exponent.

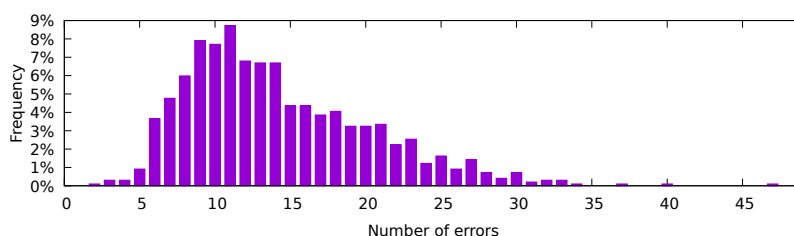


Fig. 7: Distribution of the number of errors in captured traces.

However, capture errors do occur, as shown in [Figure 7](#). To correct these, we capture multiple traces of signatures using the same private key. On average there are 14 errors in a captured trace. We find that in most cases, manually aligning traces and using a simple majority rule is sufficient to recover the complete square-and-multiply sequence. In all of the cases we have tried, combining twenty sequences yielded the complete sequence.

Acknowledgments

Yuval Yarom performed part of this work as a visiting scholar at the University of Pennsylvania. This work was supported by the Netherlands Organisation for Scientific Research (NWO) under grant 639.073.005; by the Commission of the European Communities through the Horizon 2020 program under project number 645622 (PQCRYPTO) and project number 645421 (ECRYPT-CSA); by the National Science Foundation under grants 1314919, 1408734, 1505799, 1513671, 1319880 and 14-519. by a gift from Cisco; by an Endeavour Research Fellowship from the Australian Department of Education and Training; by the 2017-2018 Rothschild Postdoctoral Fellowship; by the Blavatnik Interdisciplinary Cyber Research Center (ICRC); by the Check Point Institute for Information Security; by the Israeli Centers of Research Excellence I-CORE program (center 4/11); by the Leona M. & Harry B. Helmsley Charitable Trust; by the Warren Center for Network and Data Sciences; by the financial assistance award 70NANB15H328 from the U.S. Department of Commerce, National Institute of Standards and Technology; and by the Defense Advanced Research Project Agency (DARPA) under Contract #FA8650-16-C-7622.

Permanent ID of this document: 8016c16382e6f3876aa03bef6e4db5ff. Date: 2017.06.26.

Bibliography

- [1] GnuPG Frontends, . URL https://www.gnupg.org/related_software/frontends.html.
- [2] GNU Privacy Guard, . URL <https://www.gnupg.org>.
- [3] Thomas Allan, Billy Bob Brumley, Katrina Falkner, Joop van de Pol, and Yuval Yarom. Amplifying side channels through performance degradation. In *32nd Annual Computer Security Applications Conference (ACSAC)*, Los Angeles, CA, US, December 2016.
- [4] Naomi Benger, Joop van de Pol, Nigel P. Smart, and Yuval Yarom. “Ooh aah. . . , just a little bit”: A small amount of side channel can go a long way. In *Workshop on Cryptographic Hardware and Embedded Systems (CHES)*, pages 75–92, Busan, KR, September 2014.
- [5] Leon Groot Bruinderink, Andreas Hülsing, Tanja Lange, and Yuval Yarom. Flush, Gauss, and Reload – A cache attack on the BLISS lattice-based signature scheme. In *CHES*, volume 9813 of *LNCS*, pages 323–345. Springer, 2016.
- [6] J. Callas, L. Donnerhacke, H. Finney, D. Shaw, and R. Thayer. OpenPGP message format. RFC 4880, November 2007.
- [7] Don Coppersmith. Small solutions to polynomial equations, and low exponent RSA vulnerabilities. *J. Cryptology*, 10(4):233–260, 1997.
- [8] Christophe Doche. Exponentiation. In *Handbook of Elliptic and Hyperelliptic Curve Cryptography.*, pages 144–168. Chapman and Hall/CRC, 2005. doi: 10.1201/9781420034981.pt2.
- [9] Daniel Genkin, Adi Shamir, and Eran Tromer. RSA key extraction via low-bandwidth acoustic cryptanalysis. In *CRYPTO 2014*, pages 444–461 (vol. 1). Springer, 2014. Extended version: Cryptology ePrint Archive, Report 2013/857.
- [10] Daniel Genkin, Lev Pachmanov, Itamar Pipman, and Eran Tromer. Stealing keys from PCs using a radio: Cheap electromagnetic attacks on windowed exponentiation. In *CHES 2015*, pages 207–228, 2015. Extended version: Cryptology ePrint Archive, Report 2015/170.
- [11] Daniel Gruss, Raphael Spreitzer, and Stefan Mangard. Cache template attacks: Automating attacks on inclusive last-level caches. In *24th USENIX Security Symposium*, pages 897–912, Washington, DC, US, August 2015.
- [12] Nadia Heninger and Hovav Shacham. Reconstructing RSA private keys from random key bits. In *CRYPTO*, volume 5677 of *LNCS*, pages 1–17. Springer, 2009.
- [13] Mehmet Sinan İnci, Gorka Irazoqui, Berk Gülmezoğlu, Thomas Eisenbarth, and Berk Sunar. Cache attacks enable bulk key recovery on the cloud. In *Cryptographic Hardware and Embedded Systems (CHES)*, Santa Barbara, CA, US, August 2016.
- [14] Gorka Irazoqui, Mehmet Sinan İnci, Thomas Eisenbarth, and Berk Sunar. Wait a minute! a fast, cross-VM attack on AES. In *Symposium on Research*

- in *Attacks, Intrusions and Defenses (RAID)*, pages 299–319, Gothenburg, Sweden, September 2014.
- [15] Marc Joye and Sung-Ming Yen. Optimal left-to-right binary signed-digit recoding. *IEEE Trans. Computers*, 49(7):740–748, 2000. doi: 10.1109/12.863044.
 - [16] Fangfei Liu, Yuval Yarom, Qian Ge, Gernot Heiser, and Ruby B. Lee. Last-level cache side-channel attacks are practical. In *IEEE Symposium on Security and Privacy 2015*. IEEE, 2015.
 - [17] Alfred J. Menezes, Paul C. van Oorschot, and Scott A. Vanstone. *Handbook of Applied Cryptography*. CRC Press, October 1996.
 - [18] J.J. Moder and S.E. Elmaghraby. *Handbook of operations research: models and applications*. Number v. 1. Van Nostrand Reinhold Co., 1978.
 - [19] Kenneth G. Paterson, Antigoni Polychroniadou, and Dale L. Sibborn. *A Coding-Theoretic Approach to Recovering Noisy RSA Keys*, pages 386–403. Springer, 2012.
 - [20] Joop van de Pol, Nigel P. Smart, and Yuval Yarom. Just a little bit more. In *Cryptographers’ track at the RSA Conference on Topics in Cryptology (CT-RSA)*, pages 3–21, San Francisco, CA, USA, April 2015.
 - [21] Alfréd Rényi. On measures of entropy and information. In *Proceedings of the Fourth Berkeley Symposium on Mathematical Statistics and Probability*, volume 1, pages 547–561, Berkeley, Calif., 1961.
 - [22] Sheldon Mark Ross. *Stochastic processes*. Probability and mathematical statistics. Wiley, 1983. ISBN 0-471-09942-2.
 - [23] Colin D. Walter. Longer keys may facilitate side channel attacks. In *Selected Areas in Cryptography (SAC)*, pages 42–57, Waterloo, ON, CA, August 2004.
 - [24] Yuval Yarom. Mastik: A micro-architectural side-channel toolkit. <http://cs.adelaide.edu.au/~yval/Mastik/Mastik.pdf>, September 2016.
 - [25] Yuval Yarom and Naomi Benger. Recovering OpenSSL ECDSA nonces using the FLUSH+RELOAD cache side-channel attack. Cryptology ePrint Archive, Report 2014/140, February 2014.
 - [26] Yuval Yarom and Katrina Falkner. FLUSH+RELOAD: a high resolution, low noise, L3 cache side-channel attack. In *25th USENIX Security Symposium*, pages 719–732, San Diego, CA, US, 2014.
 - [27] Yuval Yarom, Daniel Genkin, and Nadia Heninger. CacheBleed: A timing attack on OpenSSL constant time RSA. In *Cryptographic Hardware and Embedded Systems (CHES)*, pages 346–367. Springer, 2016.
 - [28] Yinqian Zhang, Ari Juels, Michael K. Reiter, and Thomas Ristenpart. Cross-VM side channels and their use to extract private keys. In *19th ACM Conference on Computer and Communications Security (CCS)*, pages 305–316, Raleigh, NC, US, October 2012.
 - [29] Yinqian Zhang, Ari Juels, Michael K. Reiter, and Thomas Ristenpart. Cross-Tenant side-channel attacks in PaaS clouds. In *Computer and Communications Security (CCS)*, Scottsdale, AZ, US, 2014.